Preprint Cambridge Centre for Computational Chemical Engineering ISSN 1473 – 4273

Aromatic penta-linked hydrocarbons in soot nanoparticle formation

Laura Pascazio[1], Jacob W. Martin[1], Angiras Menon[1], Dingyu Hou[2,3], Xiaoqing You[2,3] and Markus Kraft[1,4,5]

released: 7 November 2019

[1] Department of Chemical Engineering and Biotechnology
University of Cambridge
West Site, Philippa Fawcett Drive
Cambridge, CB3 0AS
United Kingdom
E-mail: mk306@cam.ac.uk

[2] Center for Combustion Energy
Tsinghua University
Beijing, 100084
China

[3] Key Laboratory for Thermal Science and Power Engineering of Ministry of Education
Tsinghua University
Beijing, 100084
China

[4] School of Chemical and Biomedical Engineering
Nanyang Technological University
62 Nanyang Drive
Singapore, 637459

[5] Cambridge Centre for Advanced Research and Education in Singapore (CARES)
CREATE Tower
1 Create Way
Singapore, 138602

Preprint No. 254

Keywords: soot formation, molecular dynamics, localized π-radical, aromatic rim-bonded hydrocarbons, aromatic penta-linked hydrocarbons

Edited by
Computational Modelling Group
Department of Chemical Engineering and Biotechnology
University of Cambridge
West Site, Philippa Fawcett Drive
Cambridge, CB3 0AS
United Kingdom

Fax: + 44 (0)1223 334796
E-Mail: c4e@cam.ac.uk
World Wide Web: http://como.cheng.cam.ac.uk/

Abstract

A new crosslinking reaction between two pentagonal rings around the periphery of planar pericondensed aromatic molecules is proposed and its impact on soot nanoparticle formation explored. The reaction mechanism was computed, using density functional theory, between an aryl-type σ-radical on a rim-based pentagonal ring attacking another rim-based pentagonal ring. A hydrogen migration allowed for the formation of a double bond forming a planar aromatic penta-linked hydrocarbon (APLH) complex, recently experimentally observed. The clustering of this planar species is compared with a pericondensed polyaromatic hydrocarbon (PCAH) and an aromatic aryl-linked hydrocarbon (AALH) using molecular dynamics and metadynamics. Similar clustering is found for the investigated species compared with a pericondensed structure of similar mass indicating enhanced physical interactions after forming the crosslink. Finally, a further crosslink is possible between the unsaturated pentagonal ring sites forming an aromatic rim-linked hydrocarbon (ARLH) complex of considerable stability. This was confirmed by simulating the stable molecular dynamics of such a complex with on-the-fly quantum forces from a quantum semi-empirical method, revealing the importance of novel crosslinking reactions in soot formation.

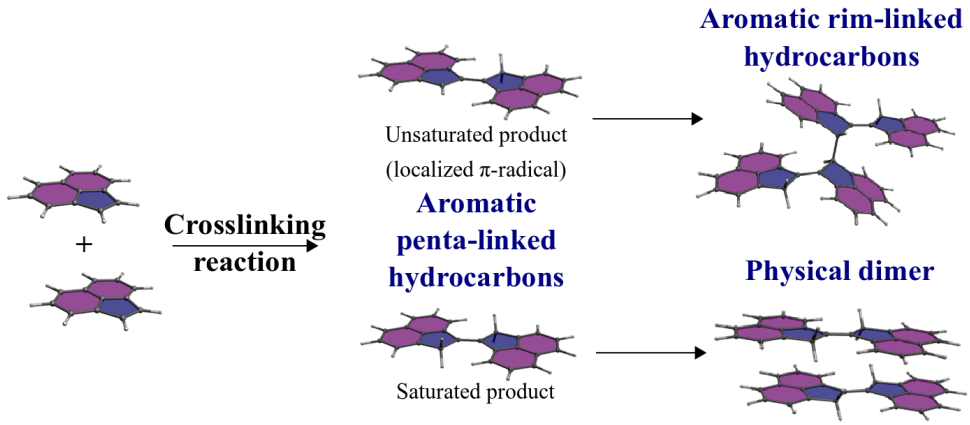

Highlights

- A new crosslinking reaction between two pentagonal rings around the periphery of aromatic molecules is proposed to produce a planar aromatic penta-linked hydrocarbon (APLH) complex.
- The physical and chemical dimerizations of the APLH are investigated using different modeling techniques.
- The APLH clusters as effectively as a pericondensed species of the same size.
- The APLH radicals can chemically dimerize forming a π-stacked and covalently bonded aromatic rim-linked hydrocarbon complex of considerable stability.

Contents

1 Introduction

Carbon particulate pollution leads to respiratory diseases, contributes to global warming while in the atmosphere and leads to increased sea ice loss through reduced albedo [2, 17, 19]. Much research has been focused on understanding the formation mechanism of soot in order to reduce the amount produced by human activities. The critical stage of particulate formation, which remains the least well understood, is the inception of gas phase aromatics to form condensed clusters of soot nanoparticles [25].

Soot forms too rapidly to be purely due to chemical reactions and must form through second order processes such as physical aggregation [9]. Mass spectrometry indicates that pericondensed polyaromatic hydrocarbons (PAH) are the primary species in flames and the first suggested explanation of rapid soot formation was physical aggregation of these large aromatics through dispersion interactions. However, *ab initio* and molecular dynamics (MD) calculations have indicated that for the size of aromatics experimentally found in flames (approximately 15 rings [4]), the intermolecular forces are insufficient for them to cluster at flame temperatures where soot forms [22].

While chemical reactions alone cannot explain soot formation, mass spectrometry has indicated that crosslinking reactions form larger PAH in sooting flames. Studying the formation of soot and fullerenes in low pressure flames using mass spectrometry [11], found evidence for a crosslink reaction forming aromatic oligomers or aromers. More recent mass spectrometry has confirmed the presence of a crosslinked species (30–50 carbon atoms) containing two smaller aromatic fragments (10–20 carbon atoms) with hydrogen to carbon ratios indicating pericondensed species [6]. This formation of aromers was found to correspond to the transition between a non-sooting and sooting flame in a low pressure methane burner, indicating the aromer formation and subsequent rearrangements are important in soot formation.

Crosslinking of PAH aryl-type σ-radicals on hexagonal rings with other PAH has previously been considered [23, 24]. Crosslinking requires the abstraction of a hydrogen atom to form the σ-radical. In most schemes, such as with aromatic aliphatically/aryl-linked hydrocarbons (AALH), a second hydrogen abstraction is required to form the stable species, which leaves the initial crosslink open to thermal fragmentation. This AALH crosslink with a hexagonal ring leads to steric interactions with the neighboring terminating hydrogen atoms, twisting the two aromatic planes of the monomers relative to each other and resulting in a non-planar crosslinked molecule. Metadynamics analysis has shown that this steric effect significantly reduces the intermolecular interactions [8]. This is due to the short range of the dispersion interactions (scaling as r^{-6}) that are easily disrupted by thermal or steric effects. Therefore, planar species are optimal for clustering due to the short range nature of dispersion interactions.

Coupling mass spectrometry with photoionisation from a tunable XUV synchrotron source has lead to a reevaluation of isomeric species present in the flame. The mass ion 202 u, for example, is often matched to the pyrene species. However, the presence of pentagon-containing fluoranthene is also required to provide the photoionisation curve for this ion [15]. Mass spectrometry also suggests a slightly higher carbon to hydrogen ratio than anticipated from D6H PAH indicating that pentagonal rings are present on the rim [6].

High resolution atomic force microscopy (HR-AFM) was able to directly image some PAH found in nearly-sooting flames and confirm the presence of these rim-based pentagonal rings [5]. The authors in [5] also imaged fully- and partially- saturated rim-based pentagonal rings as well as planar crosslinked species containing a double bond between two pentagonal rings. This penta-linked crosslink was found to be planar, which might allow for more effective van der Waals clustering than the crosslinking between hexagonal rings [5]. We also recently found that the partially saturated site forms a localized π-radical of considerable reactivity using electronic structure calculations and reactivity indices [18]. This site was found to be capable of bonding and stacking into aromatic rim-linked hydrocarbons (ARLH) indicating a potentially important role in soot formation [18].

The aim of this paper is to consider crosslinking reactions between two smaller aromatics that can lead to a planar molecule. A new crosslinking reaction between two pentagonal rings around the periphery of a PAH is proposed using hybrid density functional theory. The resulting product is a localized π-radical species similar to that found in [5]. The role of these radical species that are capable of bonding and stacking is investigated using density functional theory and quantum molecular dynamics (QMD) and the physical dimerization of the saturated aromatic product is explored using well-tempered metadynamics and MD simulations.

2 Reaction mechanism

In this section, the formation mechanism of a crosslinked planar aromatic molecule with a double bond connecting two pentagonal rings on the rim of the two aromatic subunits is investigated. Figure 1 presents the potential energy diagram for the investigated formation mechanism. All the molecular structures of stable chemical species and transition states involved in the reactions were optimized using a series of hybrid density functional calculations that we have previously benchmarked and found to provide accurate values (errors of $<$1 kcal/mol for hydrogen abstractions [12] and $<$3–7 kcal/mol for transition states in hydrocarbons). The Gaussian 09 software [10] was used to perform the geometry optimisations to determine minimum energy and transition states. Frequencies were also determined to ensure transition states possess a single imaginary frequency corresponding to the reaction.

The reaction mechanism starts with two acenaphthalene molecules (**1a** in Fig. 1). First, hydrogen abstraction by an H radical occurs, forming a σ-radical **1b** on one of the acenaphthalene pentagonal rings. This is known to be the predominant reaction mechanism for PAH growth [20]. Rim-based pentagonal rings in PAH are non-aromatic cycles. This results in strong electron localisation around the rim, and hence a very reactive site where hydrogen addition reactions can also occur (as opposed to just abstraction reactions). Low barriers are seen for hydrogen addition compared with hydrogen abstraction (see Supplementary information). However, the hydrogen addition reaction is highly reversible compared to the abstraction reaction, and thus the abstraction is still expected to proceed. The abstraction reaction from a rim-based pentagonal ring has an energy barrier of 19.5 kcal/mol compared to 16.5 kcal/mol for abstraction from the hexagonal ring. This

difference of 3 kcal/mol in barrier height can reduce the likelihood of H-abstraction from the pentagonal ring compared to the hexagonal ring at low temperatures, though the effect would be less evident at high temperatures. After the abstraction, a single bond forms between the radical site of **1b** and the carbon atom of the pentagonal ring of **1a** with a low energy barrier (1.8 kcal/mol) to form a highly stable intermediate, **1c**. Finally, a hydrogen migration from the crosslinked carbon of the pentagonal ring to the neighboring edge carbon in **1c** allows for the formation of a double bond. This forms a highly stable planar complex **1d** without requiring a subsequent hydrogen abstraction, which we call an aromatic penta-linked hydrocarbon (APLH). There is a potential chain reaction that could occur if the structure contains two or more pentagonal rings. Subsequent hydrogen abstraction on another rim-based pentagonal ring would form another σ-radical able to attack a third PAH, however, given the barrier for hydrogen abstraction we doubt such a mechanism would provide a significant nucleation flux. However, like the reaction with resonantly stabilized radicals, it would only require a single hydrogen abstraction [14]. Another interesting aspect of species **1d** is that it has a partially saturated rim-based pentagonal ring. Therefore, it forms a localized π-radical species as we have previously shown [18]. This species can then follow two routes, as detailed below: 1) the radical site can be protonated forming a closed shell species that can physically dimerize or, 2) it can stay in its radical form and chemically dimerize with another localized π-radical.

3 Physical dimerization of aromatic penta-linked hydrocarbons

The physical dimerization of the protonated closed-shell APLH discussed above was explored using well-tempered metadynamics and MD simulations. These two techniques give different information about the process. Well-tempered metadynamics is able to determine the thermodynamic stability of atomic and molecular systems and maps the free energy surfaces of the system considered, providing the minimum free energy configu-

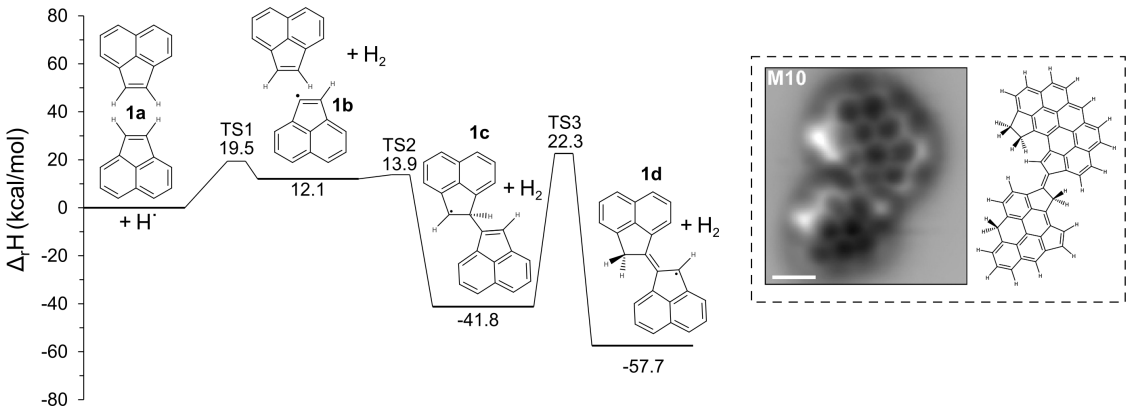

Figure 1: *Potential energy diagram for the formation of a planar crosslinked aromatic molecule with a double bond connecting rim-based pentagonal rings of the aromatic subunits at 0 K. A similar species observed experimentally has been also reported for comparison [5] used with permission CC BY-NC-ND 4.0.*

rations and the energy barriers between them. The dimerization process is investigated using this technique. However, metadynamics is not able to capture the behavior of a large system of interacting molecules. To study this, molecular dynamics calculations were run to provide some time-dependent quantities such as the size of nucleated clusters, cluster lifetimes and coagulation efficiencies at different conditions.

The clustering behaviour of a protonated APLH containing two $C_{18}H_{10}$ subunits, **2a**, is compared to two other molecules of similar sizes but different structure. In particular, **2b** also contains two $C_{18}H_{10}$ subunits but with an AALH type crosslink between two hexagonal rings, and **2c** is a pericondensed aromatic hydrocarbon (PCAH) obtained from the ring closure of the crosslinked species **2b**. The latter two kinds of molecules have previously been considered as precursor for soot nucleation [8]. The molecular mass of ≈500 u was chosen, as clustering with this periodicity has been observed in mass spectrometry studies [25]. The structures are given in Fig 2.

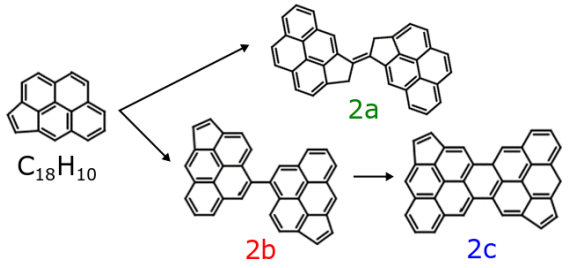

Figure 2: *Molecules considered for molecular dynamics and metadynamics simulations: a planar APLH (**2a**), an AALH (**2b**) and a PCAH (**2c**).*

The OPLS-AA forcefield was used to model the intramolecular interactions [16] and the iso-PAHAP force field [22] was used to model intermolecular interactions. The atomistic electrostatic potential charges were obtained from electronic structure calculations using the Gaussian 09 [10] program at the B3LYP/cc-pVTZ level of theory. Atom-atom non-bonded interactions were cut off at 4 nm.

3.1 Free energy profiles

The free energy (FE) calculation of the physical dimerization of these selected aromatic molecules was performed using the GROMACS 5.1 software [1] coupled with the PLUMED plugin [3] at three different temperatures (500, 1000, and 1500 K). Molecules were first minimized before starting well-tempered metadynamics simulations. Temperatures are kept constant by employing a Langevin thermostat with a time constant of 0.1 ps. Each FE profile is built as the average of three independent 100 ns runs, in which the Gaussian-shaped bias was deposited every 100 fs. The Gaussian-shaped bias had an initial width and height of 0.04 nm and 0.1 kcal/mol respectively, with bias factor set to 2.4 kcal/mol. For this process, the collective variable chosen to represent whether the system is in a monomer state or dimer state is the distance between the center of masses (COM) of the two monomers. The dimerization propensity is computed as the FE difference (ΔFE) between the dimer-state (minimum of the FE) and the monomer-state (FE calculated at long distances) according to Elvati et al. [8].

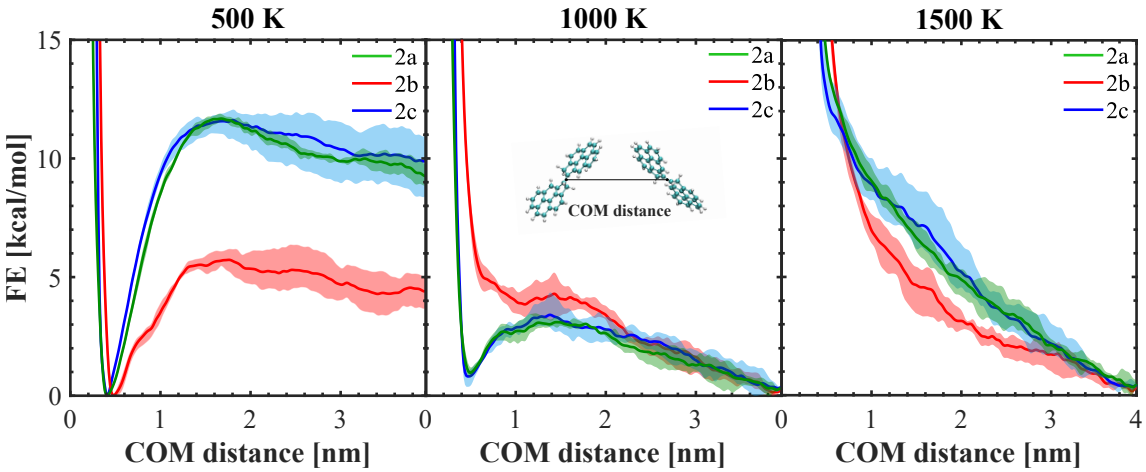

Figure 3: *Free energies (ΔFE) profiles of homodimerization of species **2a**, **2b**, and **2c** as function of the distance between centers of mass of the monomers (COM distance) at 500 K, 1000 K and 1500 K. Variation between runs are indicated by the shaded areas.*

Figure 3 reports the computed free energies of homodimerization of molecules **2a**, **2b**, and **2c** as function of the distance between centers of mass of the monomers at 500 K, 1000 K, and 1500 K. The FE profiles for all the investigated compounds do not show any dimerization propensity at 1500 K (no local minimum found in the FE profile) indicating that the entropic term dominates, in accordance with previous results reported in literature for molecules of similar sizes [7]. The dimer-state is found to be favored over the monomer-state only at 500 K for all the investigated molecules. In the temperature range 500 K–1000 K **2a** and **2c** bind more strongly than **2b** despite all three being of similar sizes. This behaviour is likely related to the planarity of the molecules and it suggests that the presence of the σ-bond in **2b** destabilizes the dimer because the two aromatic sub-units are able to rotate with respect to each other around the σ aliphatic bond. This is in agreement with previous results reported for molecules that contain an aliphatic/aryl-bond [8]. The **2a** and **2c** profiles are quite similar due to both being planar species that can maximize dispersion interactions.

Table 1: *Dimerization propensity (ΔFE) at different temperatures for the three molecules considered in this study. No values were found for 1500 K.*

Species	$\Delta FE\,(500K)$	$\Delta FE\,(1000K)$
2a	-9.81±0.3	0.9±0.1
2b	-4.46±0.5	3.85±0.9
2c	-10.12±1.2	0.81±0.5

3.2 Nucleating behaviour

The dynamic behaviour of homomolecular systems for the three PAHs reported above was analysed using MD simulations in the canonical NVT ensemble in order to observe

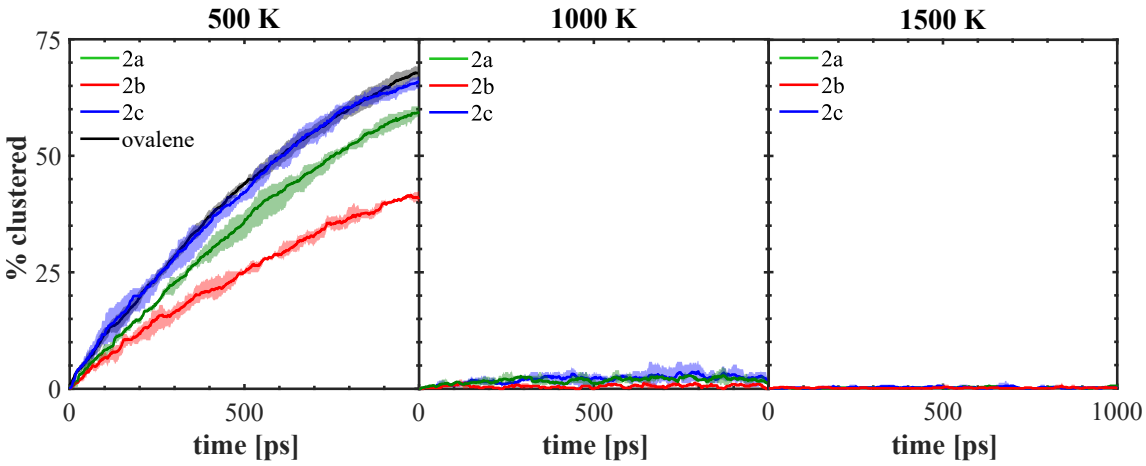

Figure 4: *Percentage of molecules in a bound state for species **2a**, **2b** and **2c** as function of the simulation time at 500, 1000 and 1500 K. Results for the ovalene case at 500 K taken from Ref. [22] are also reported for comparison. Variations between runs are indicated by the shaded areas.*

their clustering behaviour. Each simulation contained 500 molecules at a concentration of $1 \cdot 10^{18}$ cm^{-3}. A chain of ten Nosé-Hoover thermostats and a time constant of 100 fs were used to maintain a constant temperature. Three system temperatures were studied with the highest temperature corresponding to a typical flame temperature: 500 K, 1000 K, and 1500 K. Molecules were initially randomly located and orientated in a cube with periodic boundary conditions and initial velocities generated from a Maxwell-Boltzmann distribution at the given temperature. The integration time step was set to 1 fs and trajectories were integrated using the velocity Verlet algorithm. All simulations were performed using the GROMACS 5.1 software [1]. Three trajectories of 1 ns each were run for each system and the clustering data was averaged over these runs.

For identifying a cluster, we defined a cut-off distance (r_{crit} = 1.2 nm) between two molecules' centers of mass and a critical period of time (t_{crit} = 20 ps) used in previous studies [22]. This method tracks the total clustering as a function of time and evaluates clustering efficiency for a given system.

Figure 4 shows the averaged percentage of bound molecules as a function of time for each species at each temperature. As temperature increases the expected decrease is observed in the percentage of molecules bound. The maximum cluster size is also seen to reduce for all molecules (see Supplementary information). At temperatures higher than 1000 K, no significant clustering is observed, as only relatively small clusters (dimers) are formed. At 500 K much larger clusters are formed for all the systems. At 500 and 1000 K there is little difference between the clustering statistics for the two planar molecules, **2a** and **2c**, whereas the proportion of bound molecules is substantially less for **2b**, as expected from the results in Fig. 3. In Fig. 4 the results for a similar size PAH molecule (ovalene) at 500 K taken from Ref. [22] are also reported for comparison. The similar results obtained for the ovalene case and **2c** molecule thus confirm that the clustering statistics for planar PAHs are mainly dependent on the number of aromatic rings rather than their shape.

A similar trend is found for cluster lifetimes (Fig. 5). At low temperatures cluster lifetimes are generally longer and some clusters survived the whole period of simulation for all the

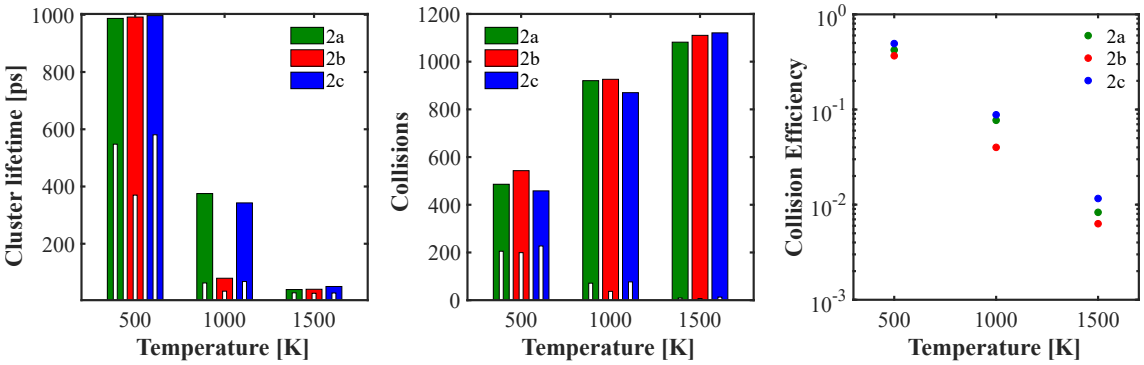

Figure 5: *Maximum lifetimes (averaged lifetimes shown in white bars) at different temperatures, overall collisions (sticking collisions shown in white bars) at different temperatures and collision efficiencies as a function of temperature for species **2a**, **2b** and **2c**.*

three species. At 1000 K, species **2a** and **2c** have an average cluster lifetimes of 548 and 581 ps, respectively, whereas species **2b** has a much lower average lifetime of 370 ps. As the temperature increases, the maximum and average lifetimes of clusters both tend to decrease for all three species. The difference between the average lifetimes of clusters for the planar **2a** and **2c** and non-planar species **2b** decreases with increasing temperature up to 1500 K, where they all have similar values (≈28 ps).

Finally, the collision efficiencies for each system are shown in Fig. 5. The collision efficiency is defined as the ratio of successful collisions (i.e. collisions which form clusters) to the total number of collisions and it is one of the key model quantities that determines the soot inception and growth rates. The collision efficiencies follow a similar trend to the cluster lifetime. At the lower temperature of 500 K, all three species have high collision efficiencies and thus successfully form clusters. At 1000 K, we observe that the planar species **2a** and **2c** have very similar collision efficiencies of 0.08 and 0.09, whilst the non-planar **2b** has a significantly lower collision efficiency of 0.04. At higher temperatures, the collision efficiency of **2c** is noticeably lower, being between **2a** and **2b**. This is likely a consequence of all three species having much lower collision efficiencies at 1500 K, which is consistent with lower average cluster lifetimes. We expect that the physical interaction will not change between the saturated species and its localized π-radical form and that the results derived from the saturated molecules can be applied to the localized π-radical species. In conclusion, physical dispersion forces are insufficient to stably bind clusters of aromatic species at flame temperatures.

4 Chemical dimerization of aromatic penta-linked hydrocarbon localized π-radicals

While the physical interaction appears to be unable to justify soot nucleation, the localized π-radical can form a chemical bond after physical dimerization. These localized π-radicals on rim-based pentagonal rings were recently found to form strongly bound

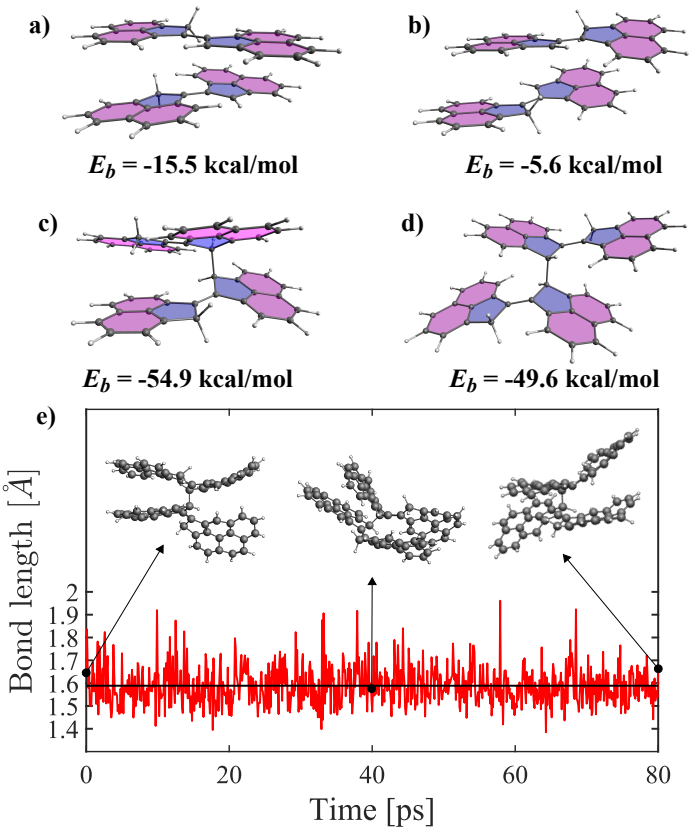

Figure 6: *a) – d) Structures with calculated binding energies M06-2X-D3/cc-pVTZ. e) Snapshots of the QMD of species c).*

stacked complexes, indicating a potentially important role in soot formation [18]. In this section, we aim to explore the crosslinking between two **1d** species and the formation of an ARLH complex. The stability of the crosslinks formed is systematically determined by calculating the binding energies using the dispersion corrected hybrid density functional M06-2X-D3/cc-pVTZ as reported in Ref. [18]. It should also be mentioned that we found that this level of theory systematically overbinds the dispersion interactions in PAH by 6±1 kcal/mol compared with SAPT(DFT) reference calculations. The binding energies of both purely physical APLH dimers and the cis and trans configurations of the chemically bound ARLH complex are reported in Fig. 6. The chemical bond in the ARLH increases considerably the binding energy between the monomers (Fig. 6a and b) compared to the physical interactions (Fig. 6c and d), 39.4 and 44 kcal/mol for the cis and trans complexes, respectively. Due to the high reactivity of radical species, the lifetimes of the physical dimers found in the previous section at 1500 K (≈28 ps) might be long enough to ensure the formation of an ARLH complex. This chemical bond could then provide the stability necessary for subsequent evolution into soot nanoparticles via another activated localized π-radical.

Finally, QMD simulations are computed with on-the-fly quantum forces using AMS2019-MOPAC software [13] to confirm the high stability of the bonded complex. This method allows us to examine, in a more realistic manner, the dynamics of the chemical dimer at

high temperatures. The semi-empirical parametric method 7 (PM7) Hamiltonian [21] was used as the interatomic manybody potential, which includes an empirical dispersion correction. Semi-empirical methods are quantum mechanical in nature, and thus preferable to classical forcefields because they represent atomic interaction forces more realistically allowing bond breaking and forming. A force field benchmark is reported in the supplementary information. At each MD simulation time step, self-consistent-field convergence of PM7 wavefunctions was achieved. A velocity Verlet integrator is used with a time step of 0.5 fs. The molecule was firstly equilibrated at a temperature of 1500 K with a 5 ps MD run, during which the temperature was kept constant using a Nosé-Hoover thermostat. After equilibration, the simulation was conducted at 1500 K for 80 ps of simulation. The results of the simulation are reported in Fig. 6e. The ARLH is stable throughout the 80 ps with a mean value of the length of the bond between APLH molecules centered at 1.589 Å.

5 Conclusion

In this work, a new crosslinking reaction mechanism between pentagonal rings on the rim of planar pericondensed PAH is proposed. The physical and chemical dimerization of the resulting planar APLH is investigated using different modeling techniques. The APLH has a similar clustering behaviour to a planar pericondensed PAH of equivalent mass indicating enhanced physical interactions after forming the double-bond crosslink, however insufficient clustering was found at flame temperatures. Finally, the APLH radical can chemically dimerize by forming a bond between the unsaturated pentagonal ring sites. This gives an ARLH forming a π-stacked and covalently bonded complex of considerable stability. This was confirmed by simulating the molecular dynamics of such a complex with quantum on-the-fly forces revealing the potential of novel crosslinking reactions and penta/rim-linked aromatics in soot formation.

Acknowledgments

This project is supported by the National Research Foundation (NRF), Prime Minister's Office, Singapore under its Campus for Research Excellence and Technological Enterprise (CREATE) programme. This project has received funding from the European Union's Horizon 2020 Research and Innovation Programme under grant agreement no. 724145. This work used the ARCHER UK National Supercomputing Service (http://www.archer.ac.uk).

A Supplementary Material

A.1 Radical generation mechanism

The generation of the σ- and π-radicals on a rim-based pentagonal ring reaction mechanism are computed and shown in Figure 7.

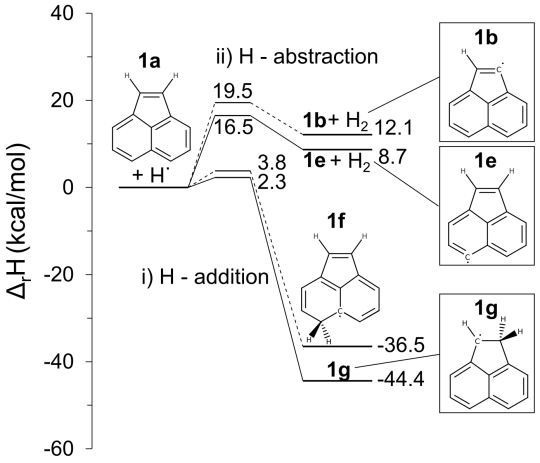

Figure 7: *Reaction mechanism computed at the M06-2X/6-311G(d,p)//B3LYP/6-311G(d,p) level of theory at 0 K.*

A.2 Molecular dynamics simulation: Maximum cluster sizes

The averaged maximum cluster sizes are shown in Figure 8. For all the system considered, increasing temperature reduces the averaged maximum cluster sizes. The results do not vary significantly between the different systems considered.

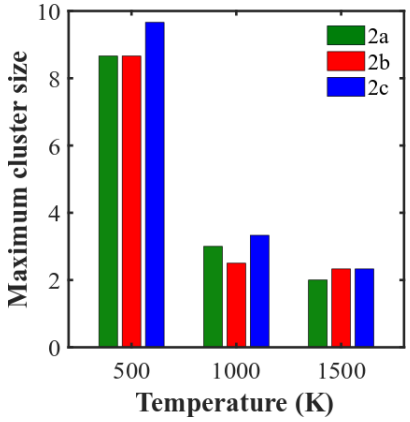

Figure 8: *Averaged maximum cluster sizes for species **2a**, **2b** and **2c** at 500 K, 1000 K and 1500 K.*

A.3 Forcefield benchmark for QMD

Molecular dynamics were performed with quantum on-the-fly forces computed using the quantum semiempirical parametric method 7 (PM7). We here have provided some benchmarking on the complexes finding a dissociation energy of -44.3 kcal/mol compared to - 49.6 kcal/mol for the M06-2X-D3 calculations indicating PM7 underbinds compared with the DFT method. This will suffice to do a preliminary exploration of dynamic stability of the aromatic rim-linked hydrocarbon formed from two penta-linked aromatics.

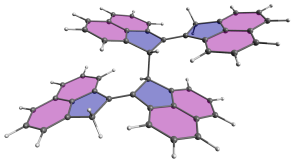

DFT: M06-2X-D3 **PM7**

E_b **= -49.6 kcal/mol** E_b **= -44.3 kcal/mol**

Figure 9: *Binding energies calculated with DFT (M06-2X-D3/cc-pVTZ) and PM7 for the* ***1d-1d*** *chemical dimer.*

References

[1] M. J. Abraham, T. Murtola, R. Schulz, S. Páll, J. C. Smith, B. Hess, and E. Lindahl. Gromacs: High performance molecular simulations through multi-level parallelism from laptops to supercomputers. *SoftwareX*, 1:19–25, 2015.

[2] T. C. Bond, S. J. Doherty, D. W. Fahey, P. M. Forster, T. Berntsen, et al. Bounding the role of black carbon in the climate system: A scientific assessment. *J. Geophys. Res.:Atmospheres*, 118(11):5380–5552, 2013. doi:10.1002/jgrd.50171.

[3] M. Bonomi, D. Branduardi, G. Bussi, C. Camilloni, D. Provasi, D. Raiteri, D. Donadio, F. Marinelli, F. Pietrucci, R. A. Broglia, and M. Parrinello. PLUMED: a portable plugin for free energy calculations with molecular dynamics. *Comp. Phys. Comm.*, 180:1961, 2009.

[4] M. L. Botero, E. M. Adkins, S. González-Calera, H. Miller, and M. Kraft. PAH structure analysis of soot in a non-premixed flame using high-resolution transmission electron microscopy and optical band gap analysis. *Combust. Flame*, 164:250–258, feb 2016. doi:10.1016/j.combustflame.2015.11.022.

[5] M. Commodo, K. Kaiser, G. De Falco, P. Minutolo, F. Schulz, A. D'Anna, and L. Gross. On the early stages of soot formation: Molecular structure elucidation by high-resolution atomic force microscopy. *Combust. Flame*, 205:154–164, 2019.

[6] P. Desgroux, A. Faccinetto, X. Mercier, T. Mouton, D. Aubagnac Karkar, and A. El Bakali. Comparative study of the soot formation process in a "nucleation" and a "sooting" low pressure premixed methane flame. *Combust. Flame*, 184:153–166, oct 2017. doi:10.1016/j.combustflame.2017.05.034.

[7] P. Elvati and A. Violi. Homo-dimerization of oxygenated polycyclic aromatic hydrocarbons under flame conditions. *Fuel*, 222:307–311, 2018.

[8] P. Elvati, K. Turrentine, and A. Violi. The role of molecular properties on the dimerization of aromatic compounds. *Proc. Combust. Instit.*, 37(1):1099–1105, 2019.

[9] M. Frenklach. Reaction mechanism of soot formation in flames. *Phys. Chem. Chem. Phys*, 4(11):2028–2037, 2002. ISSN 14639076. doi:10.1039/b110045a.

[10] M. Frisch, G. Trucks, H. Schlegel, G. Scuseria, M. Robb, J. Cheeseman, G. Scalmani, V. Barone, B. Mennucci, G. Petersson, et al. Gaussian 09, rev. A. 02, gaussian. *Inc., Wallingford, CT*, 2009.

[11] K.-H. Homann. Fullerenes and soot formation – new pathways to large particles in flames. *Angew. Chem. Int. Ed.*, 37(18):2434–2451, 1998. doi:10.1002/(SICI)1521-3773(19981002)37:18<2434::AID-ANIE2434>3.0.CO;2-L.

[12] D. Hou and X. You. Reaction kinetics of hydrogen abstraction from polycyclic aromatic hydrocarbons by H atoms. *Phys. Chem. Chem. Phys*, 19(45):30772–30780, 2017. doi:10.1039/c7cp04964a.

[13] J. James. AMS2019-MOPAC: MOPAC Engine based on the MOPAC2016 source code, http://OpenMOPAC.net. 2019.

[14] K. Johansson, M. Head-Gordon, P. Schrader, K. Wilson, and H. Michelsen. Resonance-stabilized hydrocarbon-radical chain reactions may explain soot inception and growth. *Science*, 361(6406):997–1000, 2018.

[15] K. O. Johansson, J. Zádor, P. Elvati, M. F. Campbell, P. E. Schrader, N. K. Richards-Henderson, K. R. Wilson, A. Violi, and H. A. Michelsen. Critical Assessment of Photoionization Efficiency Measurements for Characterization of Soot-Precursor Species. *J. Phys. Chem. A*, 121(23):4475–4485, 2017. doi:10.1021/acs.jpca.7b02992.

[16] G. A. Kaminski, R. A. Friesner, J. Tirado-Rives, and W. L. Jorgensen. Evaluation and reparametrization of the OPLS-AA force field for proteins via comparison with accurate quantum chemical calculations on peptides. *J. Phys. Chem. B*, 105(28): 6474–6487, 2001. doi:10.1021/jp003919d.

[17] P. J. Landrigan, R. Fuller, N. J. R. Acosta, O. Adeyi, et al. The Lancet Commission on pollution and health. *The Lancet*, oct 2017. ISSN 01406736. doi:10.1016/S0140-6736(17)32345-0.

[18] J. W. Martin, D. Hou, A. Menon, L. Pascazio, J. Akroyd, X. You, and M. Kraft. Reactivity of polycyclic aromatic hydrocarbon soot precursors: Implications of localized π-radicals on rim-based pentagonal rings. *J. Phys. Chem. C*, 123(43):26673–26682, 2019. doi:10.1021/acs.jpcc.9b07558.

[19] J. R. McConnell, R. Edwards, G. L. Kok, M. G. Flanner, C. S. Zender, E. S. Saltzman, J. R. Banta, D. R. Pasteris, M. M. Carter, and J. D. W. Kahl. 20th-Century Industrial Black Carbon Emissions Altered Arctic Climate Forcing. *Science*, 317 (5843):1381–1384, sep 2007. doi:10.1126/science.1144856.

[20] D. S. N. Parker, R. I. Kaiser, T. P. Troy, and M. Ahmed. Hydrogen abstraction/acetylene addition revealed. *Angew. Chem. Int. Ed.*, 53(30):7740–7744, 2014. ISSN 15213773. doi:10.1002/anie.201404537.

[21] J. J. P. Stewart. Optimization of parameters for semiempirical methods VI: more modifications to the NDDO approximations and re-optimization of parameters. *J. Mol. Model.*, 19(1):1–32, 2012.

[22] T. S. Totton, A. J. Misquitta, and M. Kraft. A quantitative study of the clustering of polycyclic aromatic hydrocarbons at high temperatures. *Phys. Chem. Chem. Phys*, 14(12):4081–94, 2012. doi:10.1039/c2cp23008a.

[23] A. Violi, A. Kubota, T. Truong, W. Pitz, C. Westbrook, and A. Sarofim. A fully integrated kinetic monte carlo/molecular dynamics approach for the simulation of soot precursor growth. *Proc. Combust. Instit.*, 29(2):2343–2349, 2002. doi:10.1016/S1540-7489(02)80285-1.

[24] A. Violi, A. F. Sarofim, and G. A. Voth. Kinetic Monte Carlo-molecular dynamics approach to model soot inception. *Combust. Sci. Technol.*, 176(5-6):991–1005, may 2004. ISSN 0010-2202. doi:10.1080/00102200490428594.

[25] H. Wang. Formation of nascent soot and other condensed-phase materials in flames. *Proc. Combust. Instit.*, 33(1):41 – 67, 2011. doi:10.1016/j.proci.2010.09.009.